*ELASTIC SCATTERING OF 128- AND 162-Mev NEGATIVE PIONS BY PROTONS**

Yu. A. BUDAGOV, S. WIKTOR, V. P. DZHELEPOV, P. F. ERMOLOV, and V. I. MOSKALEV

Joint Institute for Nuclear Research

Submitted to JETP editor September 18, 1959

J. Exptl. Theoret. Phys. (U.S.S.R.) **38**, 734-746 (March, 1960)

A hydrogen-filled diffusion cloud chamber in a magnetic field was used to measure the angular distribution of 128 and 162-Mev negative pions elastically scattered on protons. The total elastic scattering cross sections for these energies are $(12.8 \pm 1.0) \times 10^{-27}$ and $(21.4 \pm 1.2) \times 10^{-27}$ cm^2, respectively. The angular distribution has the form $a + b \cos\theta + c \cos^2\theta$ with the coefficients given in Sec. 5d. At the above energies the real parts of the forward scattering amplitudes (in the c.m.s.) in $\hbar/m_\pi c$ units are 0.216 ± 0.031 and 0.216 ± 0.033, respectively. These values agree with those computed from the dispersion relations with a coupling constant $f^2 = 0.08$.

1. INTRODUCTION

MUCH attention has been paid recently to an experimental verification of dispersion relations. For the scattering of charged pions by protons, the dispersion relations were obtained first by Goldberger, Miyazawa and Oehme.[1] These relations connect the real parts of the forward scattering amplitudes with the lengths of the S scattering and the integral over the total cross sections of π^+-p and π^--p interactions over the entire range of energies. In the integration interval $0 \leq \omega < \mu$ a contribution exists from the "bound state," i.e., a contribution from the neutron, as a possible intermediate state of the system in scattering. This contribution can be expressed in terms of a renormalization coupling constant f^2, characterizing the pseudo-vector interaction. The derivation of the dispersion relations is also based on general physical principles, such as the principle of microscopic causality (the requirement that there be no signals propagating with a velocity greater than that of light) and the hypothesis of charge independence of nuclear forces. The correctness of these fundamental assumptions can be verified by comparison with the experimental results. It is also possible to determine independently the coupling constant and the S-scattering lengths.

A comparison of the dispersion relation with experiment, initially performed by Anderson, Davidon, and Kruse,[2] has shown good agreement. However, in 1957 Puppi and Stanghellini[3] called attention to the fact that for negative pions one observes a discrepancy between the experimental and theoretical data. While for positive pions the real parts of the forward scattering amplitudes, determined experimentally in the energy interval up to 400 Mev, were in agreement with those calculated from the dispersion relations with a coupling constant $f^2 = 0.09 \pm 0.01$, for negative pions in the energy interval up to 200 Mev, better agreement is obtained if the coupling constant is taken to be $f^2 = 0.04$. It was shown at the same time by Agodi, Cini, and Vitale[4] that effects dependent on the charge, electromagnetic corrections, and the contribution due to hyperons and K mesons cannot explain the observed discrepancy. On the other hand, as is seen from the original work by Puppi and Stanghellini,[3] this discrepancy is based essentially on the results of one experiment — the measurements of elastic π^--p scattering by the Carnegie Institute group[5] at a π^--meson energy of 150 and 170 Mev, since the remaining experimental data have in this energy region a relatively low accuracy. In this connection, the obtaining of new experimental data on elastic π^--p scattering in the energy range from 100 to 200 Mev, and a comparison of these data with the prediction of the dispersion relations, are of undoubted interest.

In the present article we report on the measurement of elastic scattering of negative pions by protons with energies 128 and 162 Mev, obtained with the aid of a hydrogen diffusion chamber. The use of such a procedure has made it possible to avoid many specific experimental difficulties, connected with the use of electronic measurement

*This work was reported upon at the 6th session of the Scientific Council of the Joint Institute for Nuclear Research (May, 1959) and at the Conference on the Physics of High-Energy Particles in Kiev (June, 1959).

methods, and made it also possible to operate with smaller scattering angles, an important factor in the determination of the value of the differential scattering cross section at 0° angle.

2. EXPERIMENTAL CONDITIONS AND APPARATUS

Experimental setup. A diagram of the experimental setup is shown in Fig. 1. A beryllium target 3, 40 mm thick, was placed in the internal beam 2 (670 Mev) of the synchrocyclotron of the Laboratory of Nuclear Problems of the Joint Institute for Nuclear Research. The negative pions generated in the target (4) were extracted from the vacuum chamber 1 by the magnetic field,

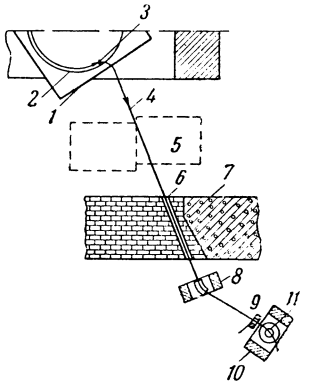

FIG. 1. Diagram of experimental setup.

passed through additional concrete shield 5, and were collimated by collimator 6, 3.6 meters long with inside diameter 50 mm, built in shielding wall 7. The negative-pion beam was then deflected by clearing magnet 8 by 40° and entered the diffusion chamber 11, placed inside electromagnet 10. An additional lead collimator 9, with a rectangular opening 350 × 50 mm, was placed in front of the chamber. The negative-pion beam was guided in the usual manner by a flexible current-carrying filament. A total of 90,000 stereophotographs was obtained with the hydrogen chamber. This material, along with the elastic π^--p scattering considered in this article, has made it possible to observe the β decay of negative pions[6] ($\pi^- \rightarrow e^- + \bar{\nu}$) and to obtain certain data on the decays of neutral pions via the schemes $\pi^0 \rightarrow e^- + e^+ + \gamma$ (reference 7) and $\pi^0 \rightarrow 2e^- + 2e^+$ (reference 8).

Diffusion chamber. The diffusion chamber was constructed to operate with light gases at pressures up to 25 atm (reference 9). A schematic diagram of this chamber, placed in a magnet, is shown in Fig. 2. The chamber is built of stainless steel and comprises a three-part vessel. In the lower (principal) part of the chamber the required temperature gradient is produced with the aid of a system of heaters and a coil carrying cooled

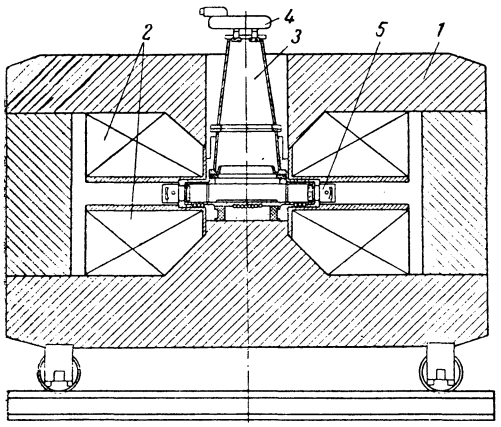

FIG. 2. Schematic diagram of the diffusion chamber, located in a solenoid magnet MS-4A. 1 – armature of electromagnet, 2 – coils, 3 – diffusion chamber, 4 – stereo camera, 5 – illuminators.

acetone. In the lower flange of the middle portion of the chamber there is a small trough for methyl alcohol, which is the working liquid of the chamber. At a bottom temperature of −70° and a trough temperature of +10° C, the temperature distribution produced in the sensitive volume of the chamber is approximately linear with a gradient of 7 deg/cm. The height of the sensitive layer becomes in this case 6 or 7 cm. The temperature is controlled and measured in various portions of the chamber with the aid of copper-constantan thermocouples.

The chamber was illuminated at an angle of 90° to the photography axis through side windows, covered with plexiglas plates 30 mm thick. These windows were mounted on the ends of rectangular projections 150 mm long, welded to the lower cylindrical portion of the chamber, so that the working diameter of the chamber (380 mm) could be increased to a maximum for the specified opening diameter of 460 mm in the upper pole of the magnet.

The chamber was illuminated by two pulsed xenon lamps IFP-500, through which 200 microfarad capacitors, charged to 2000 volts, were discharged at the instant of flash. The light from each lamp was shaped into a parallel beam by two parabolic reflectors.

The photography was by means of a stereo camera with two "Gelios-37" GOI (State Optical Institute) lenses, of 62 mm focal length; Pankhrom-X 35 mm film, with a speed of 1000 GOST units, was used. The lens resolution was 50 lines per mm in the center of the field of view. The base of the stereo camera was 120 mm, and the photographs were taken from a distance of approximately 1 mm. The necessary depth of the photographed volumes was reached at a diaphragm setting of 5.6.

The operating cycle of the camera usually lasted eight seconds. The control of the time cycle was by means of an electronic system which performed the following principal operations: a) turning on the high-frequency voltage on the dee of the synchrocyclotron for a fixed number of cycles (usually 2 — 4); b) firing the pulse lamps at a delay of 0.2 — 0.3 seconds relative to the particle pulse; c) advancing the film; d) turning the electric clearing field on and off. The necessary time delays between operations were produced by monovibrator circuits. The beam intensity was maintained by adjusting the number of cycles of acceleration in such a way that in each photograph approximately 30 negative pion tracks were registered.

Electromagnet. A constant electromagnetic field of 9000 gauss was produced in the working volume of the chamber by a solenoid magnet of type MS-4A,* designed to operate both with dc and with pulsed excitation. The magnetic field was homogeneous within 3.5% along the height of the sensitive volume of the chamber and within 2.5% along the radius. The magnetization curve and the drop in magnetic field along the height and radius of the sensitive volume were plotted with a magnetometer, operating on the Hall-effect principle.† The instrument was calibrated by the proton-resonance method.

Negative-pion beams. The average meson energy in the beam and the energy spread were determined directly by measuring the radii of curvatures of the tracks in the photographs. To reduce the track distortion due to convection currents in the chamber, the measurements were made on films exposed with the ignition of the pulsed lamp delayed by approximately half the usual time. The energies determined in this manner were (128 ± 8) and (162 ± 10) Mev, where the indicated indeterminacies represent the half width of the energy distribution of the negative pions in the chamber.

To determine the admixture of μ^- mesons and electrons in the beam, and also to monitor the energy, absorption curves in copper were plotted by means of scintillation counters. The average energies of the beam, determined by these two methods, agreed with good accuracy. The total impurity of μ^- mesons and electrons in the beams amounted to (16 ± 2) %.

*The solenoid magnet MS-4A is a modification of the MS-4 magnet. These magnets were developed at the ÉFA Scientific Research Institute by N. S. Strel'tsov, A. V. Ugamm, N. N. Indyukov, Yu. P. Semenov, V. I. Sergeeva, and A. G. Studennikova.

†The authors are grateful to D. P. Vasilevskaya and Yu. N. Denisov for allowing them to use this instrument.

3. SCANNING OF PHOTOGRAPHS AND DATA REDUCTION

The photographs obtained were scanned with stereoscopes. All the films were scanned twice by several workers independently. Some of the films were scanned a third time with particular care, to estimate the effectiveness of the double scanning, which was found to be 97%. An investigation of the angular distributions of the omitted cases has shown that this effectiveness does not depend on the specific type of scattering event (scattering angle or azimuth angle).

As a result of a double scanning, 379 scattering events were observed at 128 Mev and 1113 cases at 162 Mev. The processing of these events was carried out by the reprojection method. Both frames of the stereoscopic pair were reprojected through the same optical system, with which the photographs were taken on a screen provided with an angle-measuring device. The structure of the reprojector is analogous to that described in reference 10. For each case of scattering, the following were measured: a) coordinates of the point of interaction (x, y, z) and the coordinates z_0 of the reference marker on the bottom of the chamber; b) scattering angles of the meson, θ_π, and of the recoil proton θ_p, accurate to approximately 1°); c) azimuth angle φ of the scattering plane, accurate to approximately 2° ($\varphi = 0$ corresponds to the case when the scattering plane is horizontal); d) range of recoil proton (in those cases where this was possible).

The coordinates x, y, and z were corrected for shrinkage of the film, usually amounting to 5 — 7%. For each case this correction was determined as a ratio of the true distance from the bottom of the chamber to the principal point of the objective and that measured. The effect of film shrinkage on the measurement of angles θ and φ was very small and was neglected.

Simultaneously with processing the scattering event, we measured on the same frame the z coordinate of the track of the random negative pion. A comparison of the distributions over the altitude of the sensitive volume, h, of the scattering cases with the corresponding distributions of the same number of random tracks has shown that there was no noticeable omission in the scanning of scattering cases, located near the bottom of the chamber and near the upper boundary of the sensitive layer (Fig. 3).

For further analysis we selected the events that satisfy the following criteria:

1. The particle tracks must be coplanar accurate to 2°, i.e., the angle between any one track

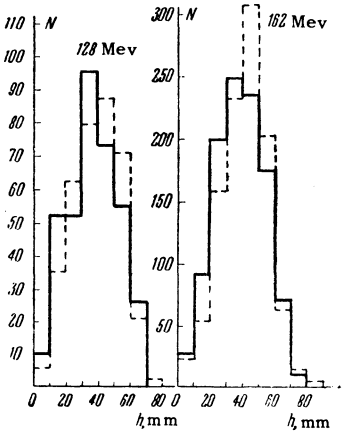

FIG. 3. Distribution of cases of elastic scattering (solid line) and of an equal number of random tracks of negative pions (dotted line) over the height h of the sensitive layer.

and the plane formed by two others must not exceed 2°.

2. The scattering angles of the negative pion and of the recoil proton should satisfy the kinematic requirements accurate to 2°; the curvatures of the tracks, the ionization density, and the recoil-proton range (in those cases when it can be measured) should also correspond to the kinematics.

3. The scattering angle of the negative pions should be more than 8° (laboratory system) (10° c.m.s.) i.e., greater than the maximum angle in $\pi^- - \mu^-$ decay.

4. The length of each of the three tracks should be not less than 5 mm.

5. The point of interaction should not be located in an insensitive region measuring more than 5 mm or obscured by an accumulation of drops measuring more than 5 mm.

6. The point of interaction should be more than 1 cm away from the chamber walls.

7. The incoming negative pions should not be deflected from the principal direction of the beam by more than 5°.

8. Cases on frames having any defects and on frames with very large intensity were disregarded.

The foregoing selection rules were satisfied by 344 scattering events at 128 Mev and 941 events at 162 Mev. All further results on the angular distributions are based on this statistical material.

4. TOTAL ELASTIC SCATTERING CROSS SECTIONS

The total elastic π^--p scattering cross sections were determined by calculating the total length of the negative pion tracks. The calculation was made in the rectangular region S, separated in the central portion of the chamber (Fig. 4). In this region we counted all the scattering events satisfying the foregoing selection criteria. The coefficients β, which take into account failures

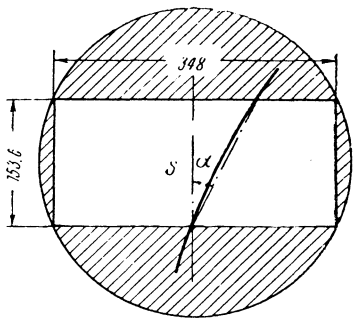

FIG. 4. Region S, separated in the chamber to calculate the total cross section of the elastic scattering.

to register cases whose scattering plane was close to vertical, were determined from the distributions over the azimuth angle φ, plotted for these cases (Fig. 5).

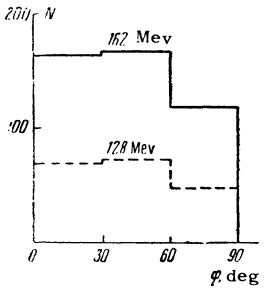

FIG. 5. Distribution of the scattering events located in region S over the aximuth angle φ.

The total number of tracks in the region S was determined by counting the tracks in all frames whose number was a multiple of 25; the resultant figure was multiplied by 25 and corrected for the number of tracks located on the frames at the end of each film. The total track length L (cm) is given by the formula

$$L = 15.36\, T\delta / \cos\alpha_{av}, \qquad (1)$$

where T is the total number of tracks, 15.36 is the width of the region S (in centimeters), α_{av} — the average angle of inclination of tracks relative to the edges of the region S (Fig. 4), and δ is a coefficient, that takes into account the substitution of a chord for the length of the arc (in our case we assumed $\delta = 1$). A correction was introduced in the total track length for broken tracks, the lengths of which were measured directly when counting the number of tracks. This correction does not exceed 4%. The total cross sections were determined from the formula

$$\sigma_{exp} = N\beta / Ln_{eff}(1 - q)\, r, \qquad (2)$$

where N and L are the number of scattering events and the total track length; n_{eff} — effective number of hydrogen nuclei in one cubic centimeter; β is the coefficient that accounts for failure to register cases with φ near to 90°; q is the impurity of μ^- mesons and electrons in the beam; r is the film scanning efficiency. Table I lists the quantities used to calculate the total cross

TABLE I. Determination of total elastic-scattering cross sections

	128 Mev		162 Mev	
	Quantity	Δ, %	Quantity	Δ,%
Number N of scattering events in the region S	190	±7.2	449	±4.7
Correction for φ inefficiency, β	1.13	±2.5	1,10	±1,5
Total number of tracks, T	$0.991 \cdot 10^6$		$1.446 \cdot 10^6$	
Total length of tracks, L	$15.3 \cdot 10^6$ cm	±1	$22.3 \cdot 10^6$ cm	±1
Effective pressure in the chamber, p_{eff}	22.5 atm		23 0 atm	
Number of nuclei per cubic centimeter, n_{eff}, at a pressure p_{eff}	$1.22 \cdot 10^{21}$ cm^{-3}	±2	$1.24 \cdot 10^{21}$ cm^{-3}	±2
Admixture of μ^- mesons and electrons in beam, q	0,16	±2	0,16	±2
Scanning efficiency, r	0,97	±1	0,97	±1
Total cross section, σ_{exp}	$14.2 \cdot 10^{-27}$ cm^2	±8.2	$22.2 \cdot 10^{-27}$ cm^2	±5.8
Total cross section of Coulomb scattering by angles $\theta > 8°$ (l.s.)	$1.6 \cdot 10^{-27}$ cm^2		$1.1 \cdot 10^{-27}$ cm^2	
Correction for scattering in the angle interval $\theta < 8°$ (l.s.)	$0.24 \cdot 10^{-27}$ cm^2		$0.35 \cdot 10^{-27}$ cm^2	
Total elastic scattering cross section, σ_{el}	$12.8 \cdot 10^{-27}$ cm^2	±8.2	$21.4 \cdot 10^{-27}$ cm^2	±5.8

sections, along with the absolute mean-square error Δ (in percent). After subtracting the Coulomb corrections from the cross sections calculated by formula (2) (the method of calculating these corrections is given in Sec. 5b) and introducing corrections for scattering in the angle interval from 0 to 8° (laboratory system) (Table I), we obtain the total cross sections of elastic π^--p scattering for 128 and 162 Mev. As can be seen from Table II, the cross sections determined in the present paper (p.p.) are in good agreement with the other experimental data.

TABLE II. Total cross sections of elastic π^--p scattering in the energy interval 100 — 200 Mev

E, Mev	σ_{el}, 10^{-27} cm^2	E, Mev	σ_{el}, 10^{-27} cm^2
98	6.15±0.22 [11]	162	21.4±1.2 (p. p.)
118	9.6±2.0 [12]	165	22.5±1.5 [15]
120	11.3±1.6 [13]	169	21.2±2.0 [16]
128	12.8±1.0 (p. p.)	170	23.5±1.0 [5]
130	12.0[14]	187	22.5±1.3 [17]
144	17.0±2.4 [13]	189	23.0±1.4 [18]
150	20.0±1.0 [5]	194	26.4±2.7 [16]
152	18.8[14]	210	28.7±3.1 [16]

5. ANGULAR DISTRIBUTION OF ELASTIC SCATTERING

The negative-pion scattering angles were recalculated in the center-of-mass system, and then all the cases were grouped in eight angle intervals of 20° each from $\theta = 10°$ to $\theta = 170°$ (c.m.s.). The scattering cases obtained in the interval $\Delta\theta = 0 - 10°$ (one case for 128 Mev and nine cases for 162 Mev) were disregarded (see selection rules, Section 3), owing to the extremely low efficiency of observation, since the recoil protons have a very small range when the mesons are scattered by $\theta < 10°$, and the scattering cases could not be distinguished from π^--μ^- decays. In addition, the Coulomb scattering cross section is very large in this angle interval. The interval $\Delta\theta = 170 - 180°$ was also disregarded owing to the low efficiency (only one case, $\theta = 173°$, was observed although the expected number was 3 to 5).

Columns 1 and 2 of Tables III and IV list the angles θ corresponding to the centers of the angle intervals, and the number of scattering cases ΔN

TABLE III. Differential cross sections of elastic π^--p scattering at 128 Mev

θ (c.m.s.)	ΔN	α	$\left(\frac{d\sigma}{d\Omega}\right)_{exp}$, 10^{-27} cm^2/sr	$\left(\frac{d\sigma}{d\Omega}\right)_{nuc}$, 10^{-27} cm^2/sr
20°	61	1.22±0.06	3.63±0.50	2.01±0.54
40°	78	1.14±0.05	2.31±0.28	2.07±0.28
60°	44	1.08±0.02	0.91±0.14	0.85±0.14
80°	37	1.08±0.02	(1.00±0.08)×0.68±0.11	(1.00±0.08)×0.66±0.11
100°	33	1.08±0.02	0.60±0.10	0.60±0.10
120°	33	1.08±0.02	0.69±0.12	0.70±0.12
140°	34	1.08±0.06	0.95±0.17	0.98±0.17
160°	23	1.25±0.10	1.40±0.31	1.43±0.31

TABLE IV. Differential cross sections of elastic π^--p scattering at 162 Mev

θ (c.m.s.)	ΔN	α	$\left(\frac{d\sigma}{d\Omega}\right)_{exp}$, 10^{-27} cm^2/sr	$\left(\frac{d\sigma}{d\Omega}\right)_{nuc}$, 10^{-27} cm^2/sr
20°	139	1.20±0.04	4.76±0.43	3.60±0.46
40°	175	1.02±0.01	2.71±0.21	2.55±0.21
60°	159	1.09±0.01	1.96±0.16	1.91±0.16
80°	96	1.09±0.01	(1.00±0.06)×1.04±0.11	(1.00±0.06)×1.02±0.11
100°	86	1.09±0.01	0.93±0.10	0.92±0.10
120°	102	1.09±0.01	1.26±0.12	1.26±0.12
140°	124	1.12±0.03	2.11±0.20	2.13±0.20
160°	60	1.20±0.06	2.06±0.28	2.09±0.28

in each interval. To obtain the differential cross sections from these data, it is necessary to take into account the failure to register cases with φ close to 90°, Coulomb corrections, and corrections for averaging over the angle interval $\Delta\theta$.

a. Corrections for φ Ineffectiveness

The scattering cases, whose planes were close to vertical ($\varphi \sim 90°$) are more likely to be omitted in the scanning than cases located in planes close to horizontal. Here obviously the effectiveness should be lower for small and for very large scattering angles θ. Figures 6 and 7 show the distributions of the scattering cases by azimuth angle φ for different angular intervals $\Delta\theta$. The registration effectiveness obtained from these distributions for events in the interval $\Delta\theta = 45 - 135°$ amounts to 92 — 93%, and drops to 80 — 83% for the angular intervals $\Delta\theta = 10 - 30°$ and $\Delta\theta = 150 - 170°$. The coefficients α, which take into account the φ ineffectiveness, are listed in column 3 of Tables III and IV.

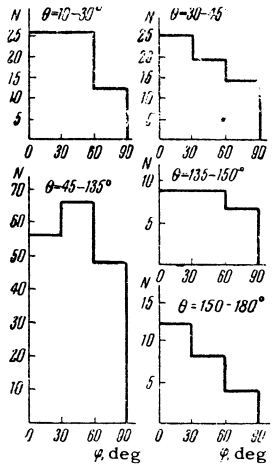

FIG. 6. Azimuthal distribution of scattering events at 128 Mev for different angular intervals $\Delta\theta$.

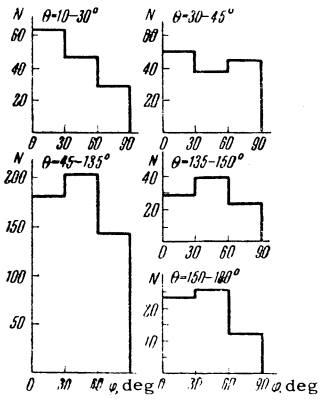

FIG. 7. Azimuthal distribution of scattering events at 162 Mev for different angular intervals $\Delta\theta$.

b. Coulomb Corrections

The Coulomb corrections were calculated using relativistic Coulomb-scattering amplitudes, obtained by Solmitz.[19] The differential scattering cross section due to Coulomb interaction can be written in the form

$$\left(\frac{d\sigma}{d\Omega}\right)_{\text{Coul+int}} = \Phi_1 \sin^{-4}\frac{\theta}{2} + \Phi_2 \sin^{-2}\frac{\theta}{2} + \Phi_3 + \Phi_4 \sin^2\frac{\theta}{2}, \tag{3}$$

where θ is the scattering angle in the c.m.s. The first term in (3) is the cross section of the pure Coulomb scattering, and the remaining terms are due to interference between the Coulomb and nuclear scatterings. The coefficients Φ are calculated from the following formulas

$$\begin{aligned}
\Phi_1 &= A^2(B+C)^2,\\
\Phi_2 &= 4A^2D^2 - 4A^2C(B+C) + A(B+C)(E+F),\\
\Phi_3 &= 4A^2(C^2-D^2) - 2AC(E+F)\\
&\quad - 2AF(B+C) - 4ADG,\\
\Phi_4 &= 4A(CF+DG),
\end{aligned} \tag{4}$$

where

$$\begin{aligned}
&A = e^2/2pc(\beta_\pi+\beta_p), \quad B = 1 + \tfrac{1}{2}\beta_\pi\beta_p - \tfrac{1}{4}\beta_p^2(2\mu_p - 1),\\
&C = \tfrac{1}{2}\beta_\pi\beta_p + \tfrac{1}{4}\beta_p^2(2\mu_p - 1),\\
&D = \tfrac{1}{2}\mu_p\beta_\pi\beta_p + \tfrac{1}{4}\beta_p^2(2\mu_p - 1), E = \tfrac{1}{3}k^{-1}(2\sin 2\alpha_1 + \sin 2\alpha_3),\\
&F = \tfrac{1}{3}k^{-1}(2\sin 2\alpha_{11} + \sin 2\alpha_{31} + 4\sin 2\alpha_{13} + 2\sin 2\alpha_{33}),\\
&G = \tfrac{1}{3}k^{-1}(2\sin 2\alpha_{13} + \sin 2\alpha_{33} - 2\sin 2\alpha_{11} - \sin 2\alpha_{31}).
\end{aligned} \tag{5}$$

In these formulas $p = \hbar k$ is the momentum in the c.m.s., β_π and β_p are the velocities of the negative pion and the proton in the c.m.s., μ_p is the magnetic moment of the proton in nuclear magnetons. We give below the values of the coefficients Φ (in 10^{-27} cm^2/sr) for negative pion energies of 128 and 162 Mev, calculated from the foregoing formulas, and use for the calculation of E, F, and G the meson-nucleon interaction phases obtained by Chiu and Lomon:[20]

	$10^4\,\Phi_1$	$10^2\,\Phi_2$	$10^2\,\Phi_3$	$10^2\,\Phi_4$
$E = 128$ Mev:	2.18	3.61	—9.33	3.21
$E = 162$ Mev:	1.54	2.57	—7.26	2.96

The integration of (3) from 10° to 180° yields the corrections to the total elastic-scattering cross sections (see Table I)

$$\sigma_{\text{Coul+int}} = 2\pi \int_{10^\circ}^{180^\circ} \left(\frac{d\sigma}{d\Omega}\right)_{\text{Coul+int}} \sin\theta d\theta = \begin{cases} 1.6\cdot 10^{-27}\ \text{cm}^2 & \text{for 128 Mev,} \\ 1.1\cdot 10^{-27}\ \text{cm}^2 & \text{for 162 Mev.} \end{cases}$$

To obtain the differential cross sections of pure nuclear scattering from the experimentally-obtained values $(d\sigma)_{exp}$, we calculated the cross sections

$$(d\sigma)_{\text{Coul+int}} = 2\pi \int_{\Delta\theta} \left(\frac{d\sigma}{d\Omega}\right)_{\text{Coul+int}} \sin\theta d\theta,$$

in which the errors were determined by varying the phase shifts that enter into (5) over reasonable limits.

c. Correction for the Averaging Over the Angular Interval $\Delta\theta$

Since the midpoint of the interval θ is assigned a cross section value which is averaged over the finite angular interval $\Delta\theta$, the true value of the cross section for the angle θ will differ from the average one by an amount

$$d(\theta) = -\tfrac{1}{24}(\Delta\theta)^2 [d\sigma(\theta)/d\Omega]'', \qquad (6)$$

where $[d\sigma(\theta)/d\Omega]''$ is the second derivative of the differential cross section. As a first approximation we calculated $d(\theta)$ from the expressions $d\sigma(\theta)/d\Omega = a' + b' \cos\theta + c' \cos^2\theta$, obtained by the least-squares method from the experimental differential cross sections, corrected for Coulomb scattering. Then

$$d(\theta) = \tfrac{1}{24}(\Delta\theta)^2 (b' \cos\theta + 2c' \cos 2\theta). \qquad (7)$$

The maximum error as calculated by formula (7) did not exceed 2.5%.

d. Differential Cross Section of Elastic Scattering

The differential cross sections $(d\sigma/d\Omega)_{exp}$ (columns 4, Tables III and IV) were obtained from the angular distributions $dN/d\Omega$ by normalization to the total cross section σ_{exp} (Table I), with allowance for the coefficients α. Columns 5 of Tables III and IV list the differential cross sections of elastic π^--p scattering, due to purely-nuclear interaction. They were obtained by subtracting from $(d\sigma/d\Omega)_{exp}$ the Coulomb-scattering cross sections and by introducing corrections for averaging over the angle intervals. These errors are mean-square errors, due principally to statistical errors and to small indeterminacies due to introduction of corrections. The general factor in front of the cross sections is the error in the normalized total cross section.

Through the experimentally obtained cross sections $(d\sigma/d\Omega)_{nuc}$, the curves of the form $d\sigma/d\Omega = a + b\cos\theta + c\cos^2\theta$ were drawn by the method of least squares. We give below the values of the coefficients a, b, and c (in 10^{-27} cm^2/sr), and also the quantity $M = \sum_i (\epsilon_i/\Delta\sigma_i)^2$ which is the sum of the squares of the deviations ϵ_i of the calculated cross sections from the experimental points, expressed in units of experimental errors $\Delta\sigma_i$, and the number of degrees of freedom $M_0 = n - m$ (n — number of experimental points, m — number of parameters of the curve). The fact that M is close to M_0 indicates good agreement between the drawn curves and the experimental cross sections

$E = 128$ Mev: $\left.\begin{matrix} a=0.55\pm0.07 \\ b=0.34\pm0.12 \\ c=1.30\pm0.24 \end{matrix}\right\} \times(1.00\pm0.08);\ M=5.8;\ M_0=5;$

$E = 162$ Mev: $\left.\begin{matrix} a=0.93\pm0.07 \\ b=0.51\pm0.12 \\ c=2.28\pm0.22 \end{matrix}\right\} \times(1.00\pm0.06);\ M=5.2;\ M_0=5.$

The error matrices $10^4 G_{ij}^{-1}$, calculated by the method given in the paper by Klepikov and Sokolov,[21] have the following form

128 Mev			162 Mev		
53.53	—3.73	—118.15	49.78	0.76	—101.65
—4.1%	153.65	86.48	0.9%	140.28	39.35
—66.3%	28.6%	593.87	—64.8%	14.9%	494.60

The errors in the coefficients a, b, and c are the square roots of the diagonal elements of the matrices. The non-diagonal elements are the products of the corresponding standard deviations, multiplied by the correlation coefficient. In one half of the matrices, the non-diagonal elements are replaced by the correlation coefficients between a, b, and c (in percent).

The curves obtained, together with the experimental points, are shown in Fig. 8. They agree with the angular distributions of elastic π^--p scattering, measured by Ashkin et al.[5] at 150 and 170 Mev, and also with the results of Kruse and Arnold[14] at negative-pion energies of 130 and 152 Mev.

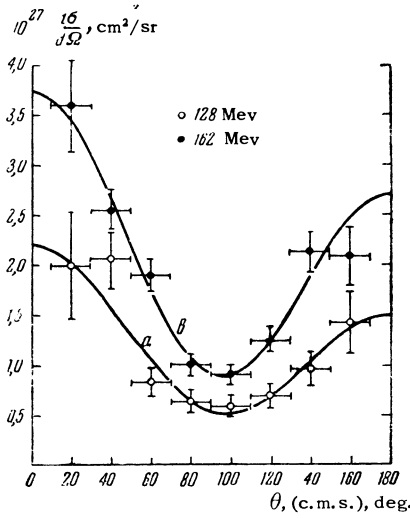

FIG. 8. Angular distributions of elastic π^--p scattering at 128 and 162 Mev. Curves a and b are found by the least-squares method with allowance for S and P waves only.

e. Determination of the Real Part of the Forward Scattering Amplitude

The differential forward-scattering cross sections $d\sigma(0)/d\Omega = a + b + c$ for 128 and 162 Mev are respectively equal to $(220 \pm 0.32) \times 10^{-27}$ and $(3.73 \pm 0.32) \times 10^{-27}$ cm²/sr. These errors take into account, in addition to the mean squared deviations of the coefficients a, b, and c, the correlation between the coefficients (non-diagonal elements of the error matrices). The magnitude of the real part of the forward-scattering amplitude $\mathrm{Re}\, f(0, \omega)$ can be readily obtained from the optical theorem

$$\mathrm{Im}\, f(0, \omega) = k\sigma_t / 4\pi, \qquad (8)$$

where σ_t is the total cross section of π^--p interaction. Then

$$D^b_- = \mathrm{Re}\, f(0, \omega) = \sqrt{\frac{d\sigma}{d\Omega}(0) - \frac{k^2}{16\pi^2}\sigma_t^2}. \qquad (9)$$

The values of σ_t were taken from the curve of the energy dependence of the total cross sections, obtained by Klepikov, Meshcheryakov, and Sokolov[22] by analyzing all the experimental data on the total cross sections of π^+-p and π^--p interactions over a wide range of energies.

$$\sigma_t\,(128\,\mathrm{Mev}) = (39.7 \pm 1.0) \cdot 10^{-27}\ \mathrm{cm}^2,$$

$$\sigma_t\,(162\,\mathrm{Mev}) = (63.3 \pm 1.0) \cdot 10^{-27}\ \mathrm{cm}^2.$$

Then the real parts of the forward-scattering amplitude in the center-of-mass system (in units of $\hbar/m_\pi c$) are

$$D^b_-\,(128\,\mathrm{Mev}) = 0.261 \pm 0.031,$$

$$D^b_-\,(162\,\mathrm{Mev}) = 0.216 \pm 0.038.$$

The great relative error in D^b_- (162 Mev) is due to the fact that the formula for the error D contains D in the denominator, and therefore when resonance is approached, as $D \to 0$, the relative error increases without limit.

6. DISCUSSION

During the performance of this experiment, several theoretical papers appeared[23-31] in which possible causes of the discrepancy observed by Puppi and Stanghellini are discussed. Zaidi and Lomon[23] have shown that the value of D^b_- depends greatly on the course of the curve of total cross sections of π^--p interaction near resonance. A detailed analysis of the errors that arise when the dispersions relations are applied to π-p scattering was carried out by Hamilton[25] and by Schnitzer and Salzman.[28] The latter have shown that by using the energy dependence obtained by Anderson[32] for the total cross sections, it is possible to reduce the discrepancy between the experimental and theoretical values of D^b_- by a factor of approximately 2. In addition, allowance for the normalization factor in the differential cross sections and for the correlation between the coefficients a, b, and c leads to an increase in the errors in the experimental values of D^b_- at 150 and 170 Mev, by a factor of approximately 2, compared with the errors indicated by Puppi and Stanghellini. In spite of this, a slight discrepancy still remains, and to explain it it is necessary to obtain more precise experimental data on the total cross section near resonance and to obtain new values of D^b_-.[28-30]

Most recently, Klepikov, Meshcheryakov, and Sokolov[22] have calculated the curve $D^b_-(\omega)$ for $f^2 = 0.08$, using new data on the total cross sections over a wide range of energies, including measured values of $\sigma_t(\pi^-\text{-p})$, accurate to 2 — 3%, obtained by Zinov, Konin, Korenchenko, and Pontecorvo[33] in the pion energy range 160 — 330 Mev. Figure 9 shows the curve by Klepikov et al. drawn with a solid line, while the dotted line represents the curve of Schnitzer and Salzman[28] for $f^2 = 0.08$. The solid bullets denote the values of D^b_- obtained in the present investigation. In addition, the figure shows recent results by Barnes et al. (41.5 Mev),[34] Edwards et al. (98 Mev),[11] and Kruse and Arnold (130 and 152 Mev),[14] and also the values of D^b_- at 150 and 170 Mev,[3] the errors of which were recal-

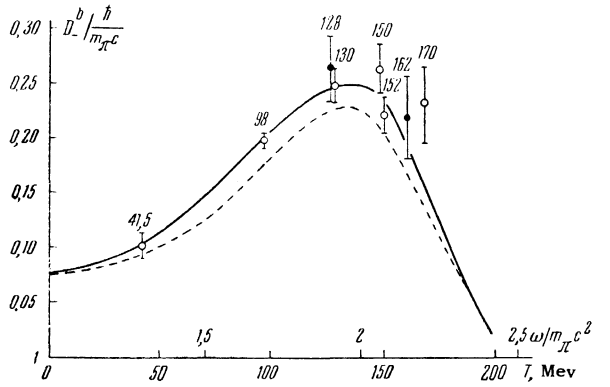

FIG. 9. Dependence of the real part of the forward scattering amplitude, D_-^b on the energy (ω – total negative-pion energy, T – kinetic energy). Solid curve – by Klepikov et al.[22] ($f^2 = 0.08$), dotted curve – by Schnitzer and Salzman[28] ($f = 0.08$).

culated by Schnitzer and Salzman.[28] As can be seen from Fig. 9, the results of our experiments and the data of all the later experimental investigations of elastic π^--p scattering in the energy range up to resonance agree quite satisfactorily with the new theoretical curve, calculated with a coupling constant $f^2 = 0.08$.

Thus, one can assume at present that the experimental data on elastic scattering of negative pions by protons also agrees with the dispersion relations at $f^2 = 0.08$, as was already established earlier for the scattering of positive pions.

The authors express their gratitude to L. I. Lapidus, S. N. Sokolov, V. A. Meshcheryakov for useful discussions, to L. I. Krasnoslobodtseva, T. S. Sazhneva, and Yu. L. Saĭkina for help in scanning the photographs, and to A. A. Andrianova and G. D. Malysheva for calculating the error matrices.

[1] Goldberger, Miyazawa, and Oehme, Phys. Rev. **99**, 986 (1955).

[2] Anderson, Davidon, and Kruse, Phys. Rev. **100**, 339 (1955).

[3] G. Puppi and A. Stanghellini, Nuovo cimento **5**, 1305 (1957).

[4] A. Agodi and M. Cini, Nuovo cimento **5**, 1256 (1957); **6**, 686 (1957); Agodi, Cini, and Vitale, Phys. Rev. **107**, 630 (1957).

[5] Ashkin, Blaser, Feiner, and Stern, Phys. Rev. **101**, 1149 (1956).

[6] Budagov, Viktor, Dzhelepov, Ermolov, and Moskalev, JETP **37**, 878 (1959), Soviet Phys. JETP **10**, 625 (1960).

[7] Budagov, Viktor, Dzhelepov, Ermolov, and Moskalev, JETP **35**, 1575 (1958), Soviet Phys. JETP **8**, 1101 (1959); JETP **38**, No. 4 (1960), Soviet Phys. JETP, in press.

[8] Budagov, Viktor, Dzelepov, Ermolov, and Moskalev, JETP **36**, 1080 (1959), Soviet Phys. JETP **9**, 767 (1959).

[9] Budagov, Viktor, Dzhelepov, Ermolov, and Moskalev, Материалы совещания по камерам Вильсона, диффузионным и пузырьковым камерам (Proceedings of the Conference on Cloud, Diffusion, and Bubble Chambers) Joint Institute for Nuclear Research, Dubna, 1958.

[10] Vasilenko, Kozodaev, Sulyaev, Filippov, and Shcherbakov, Приборы и техника эксперимента (Instrum. and Meas. Engg.) No. 6 (1957).

[11] Edwards, Frank, and Holt, Proc. Phys. Soc. **73**, 856 (1959).

[12] J. Orear, Phys. Rev. **92**, 156 (1953).

[13] Anderson, Fermi, Martin, and Nagle, Phys. Rev. **91**, 155 (1953).

[14] U. Kruse and R. Arnold, Материалы конференции по физике высоких энергий, г. Киев, Proceedings of the Conference on High-energy Physics in Kiev) July, 1959, lecture by B. M. Pontecorvo.

[15] H. L. Anderson and M. Glicksman, Phys. Rev. **100**, 268 (1955).

[16] Fermi, Glicksman, Martin, and Nagle, Phys. Rev. **92**, 161 (1953).

[17] M. Glicksman, Phys. Rev. **95**, 1045 (1954).

[18] Kruse, Anderson, Davidon, and Glicksman, Phys. Rev. **100**, 279 (1955).

[19] F. T. Solmitz, Phys. Rev. **94**, 1799 (1954).

[20] H. Y. Chiu and E. L. Lomon, Ann. Phys. **6**, 50 (1959).

[21] N. P. Klepikov and S. N. Sokolov, Analysis of Experimental Data by the Method of Maximum Likelihood, preprint, Joint Institute for Nuclear Research, 1959.

[22] Klepikov, Meshcheryakov, and Sokolov, loc. cit. ref. 14.

[23] M. H. Zaidi and E. L. Lomon, Phys. Rev. **108**, 1352 (1959).

[24] V. A. Meshcheryakov, JETP **35**, 290 (1958), Soviet Phys. JETP **8**, 200 (1959).

[25] J. Hamilton, Phys. Rev. **110**, 1134 (1958).

[26] H. Y. Chiu, Phys. Rev. **110**, 1140 (1958).

[27] L. Bertocchi and L. Lendinara, Nuovo cimento **10**, 734 (1958).

[28] H. J. Schnitzer and G. Salzman, Phys. Rev. **112**, 1802 (1959).

[29] H. Y. Chiu and J. Hamilton, Phys. Rev. Lett. **1**, 146 (1958).

[30] H. P. Noyes and D. N. Edwards, Bull. Am. Phys. Soc. **4**, 50 (1959).

[31] H. J. Schnitzer and G. Salzman, Phys. Rev. **113**, 1153 (1959).

[32] H. L. Anderson, Proc. of the Sixth Ann. Roch. Conf., 1959 p. 20.

[33] Zinov, Konin, Korenchenko, and Pontecorvo, loc. cit. ref. 14.

[34] Barnes, Rose, Giacomelli, Ring, and Miyake, Phys. Rev., in press.

Translated by J. G. Adashko
148